The Canadian Mineralogist
Vol. 51, pp. 93-106 (2013)
DOI: 10.3749/canmin.51.1.93

WOPMAYITE, IDEALLY $Ca_6Na_3\square Mn(PO_4)_3(PO_3OH)_4$, A NEW PHOSPHATE MINERAL FROM THE TANCO MINE, BERNIC LAKE, MANITOBA: DESCRIPTION AND CRYSTAL STRUCTURE

MARK A. COOPER, FRANK C. HAWTHORNE, YASSIR A. ABDU AND NEIL A. BALL

Department of Geological Sciences, University of Manitoba, Winnipeg, MB, R3T 2N2, Canada

ROBERT A. RAMIK AND KIMBERLY T. TAIT

Department of Natural History, Mineralogy, Royal Ontario Museum, 100 Queen's Park, Toronto, Ontario M5S 2C6, Canada

ABSTRACT

Wopmayite, ideally $Ca_6Na_3\square Mn(PO_4)_3(PO_3OH)_4$, is a new secondary mineral from the Tanco mine, Bernic Lake, Manitoba. It occurs in vugs in a single 5–10 cm mass of phosphate-carbonate mineralization in a spodumene-rich boulder found in the dumps of the Tanco Mine, Bernic Lake, Manitoba, Canada. It is a secondary mineral that crystallized together with rhodochrosite, quartz, whitlockite, apatite, and other phases after dissolution of primary lithiophosphate by hydrothermal solutions. The initial crystal of wopmayite was a corroded $\{10\bar{1}1\}$ rhomb ~150 microns across. Wopmayite is colorless to white to pale pink with a white streak and a vitreous luster, and does not fluoresce under ultraviolet light. It has a Mohs hardness of 5, is brittle, has an irregular to subconchoidal fracture, and shows no cleavage or parting. The calculated density is 3.027 g/cm^3. It is uniaxial (–), ω = 1.617, ε = 1.613, both ± 0.002. Wopmayite is hexagonal-rhombohedral, space group *R*3*c*, *a* 10.3926(2), *c* 37.1694(9) Å, *V* 3476.7(2) Å^3, Z = 6, *a*:*c* = 1:3.577. The seven strongest lines in the X-ray powder-diffraction pattern are as follows: *d* (Å), *I*, (*h k l*): 2.858, 100, (02.10); 3.186, 88, ($\bar{2}34$); 2.589, 68, ($\bar{2}40$); 5.166, 33, ($\bar{1}20$); 6.421, 32, ($\bar{1}14$); 8.017, 31, (012); and 3.425, 29, ($\bar{1}110$). Chemical analysis by electron microprobe gave P_2O_5 46.40, Al_2O_3 0.38, Fe_2O_3 0.80, FeO 0.96, MnO 3.74, MgO 0.41, CaO 37.65, SrO 0.91, Na_2O 5.43, and H_2O(calc) 2.00, sum 98.68 wt.%. The H_2O content was determined by crystal-structure analysis. On the basis of 28 O *apfu*, the empirical formula is $(Ca_{7.19}Na_{1.88}Sr_{0.09})_{\Sigma 9.16}(Mn_{0.56}Mg_{0.11}Fe^{2+}_{0.14}Fe^{3+}_{0.11}Al_{0.08})_{\Sigma 1.00}(PO_4)_{4.63}(PO_3OH)_{2.37}$, and the endmember formula is $Ca_6Na_3\square Mn(PO_4)_3(PO_3OH)_4$.

The crystal structure of wopmayite was solved by direct methods and refined to an R_1 index of 2.21% based on 2288 unique observed reflections collected on a three-circle rotating-anode (Mo$K\alpha$ X-radiation) diffractometer equipped with multilayer optics and an APEX-II detector. Wopmayite has a structural unit consisting of an $[M^{2+}(PO_4)_6]$ arrangement that is topologically the same as the structural units in the whitlockite and merrillite structures. The $[M^{2+}(PO_4)_6]$ clusters are linked by Ca polyhedra and $(PO_3\Phi)$ groups of the form $\{Ca_9X(PO_3\Phi)\}$ where Φ = O,OH and *X* = ($\square$, Na, Ca), depending on the mineral species. Wopmayite is related to whitlockite by the substitution Na + H → Ca + $\square$, whereby Na is incorporated primarily at the *Ca*(3) site and H attaches to the *P*(1) tetrahedron to produce an acid-phosphate group. Thus merrillite contains no acid-phosphate group, whitlockite contains a single acid-phosphate group at *P*(3), and wopmayite contains acid-phosphate groups at both *P*(1) and *P*(3).

Keywords: Wopmayite, new mineral species, phosphate, Tanco mine, Manitoba, Canada, crystal structure, electron microprobe analysis, optical properties, powder-diffraction pattern, whitlockite, merrillite.

INTRODUCTION

The Tanco mine is located on the northwest shore of Bernic Lake, Manitoba, about 180 km east-northeast of Winnipeg, Manitoba. The geology of the Tanco pegmatite was described extensively by Stilling *et al.* (2006). Tanco is a zoned petalite-subgroup pegmatite (Černý 1991) within the Bird River Greenstone Belt of the Superior Province. Several new phosphate mineral species have been described from the Tanco pegmatite: tancoite, $HNa_2LiAl(PO_4)_2(OH)$ (Ramik *et al.* 1980, Hawthorne 1983a); ercitite, $Na_2(H_2O)_4[Mn^{3+}{}_2(OH)_2(PO_4)_2]$ (Fransolet *et al.* 2000, Cooper *et al.* 2009a); and groatite, $NaCaMn^{2+}{}_2(PO_4)[PO_3(OH)]_2$ (Cooper *et al.* 2009b). In the description of groatite, Cooper *et al.* (2009b) noted the presence of whitlockite, ideally $Ca_9Mg(PO_4)_6(PO_3OH)$, in open boxwork structures resulting from the dissolution of lithiophosphate.

§ Corresponding author, e-mail address:

Further examination of these boxwork structures showed the presence of a rhombohedral phosphate similar to whitlockite but containing significant Na. This was subsequently characterized as a new mineral species and is named wopmayite, after Wilfrid Reid "Wop" May (1896–1952) who was born in Carberry, Manitoba, Canada. "Wop" May was a pioneering aviator who created the role of the bush pilot, and opened up the Canadian North to mineral exploration and mining.

The new mineral and mineral name have been approved by the Commission on New Minerals, Nomenclature and Classification, International Mineralogical Association (IMA 2011-093). The holotype specimen of wopmayite has been deposited in the mineral collection of the Department of Natural History, Royal Ontario Museum, catalogue number M40501.

Occurrence

Wopmayite occurs in vugs in a single 5–10 cm mass of phosphate-carbonate mineralization in a spodumene-rich boulder found in the dumps of the Tanco Mine, Bernic Lake, Manitoba, Canada. The assemblage is primarily rhodochrosite, quartz, whitlockite, apatite, and fairfieldite, with lesser crandallite, calcite, overite, wopmayite, groatite, and metaswitzerite. Also of note was a small mass of sphalerite, and bismuthinite inclusions within rhodochrosite. Surficially altered spodumene crystals penetrate into the mineralization. Wopmayite is a secondary mineral that crystallized together with rhodochrosite, quartz, whitlockite, apatite, and other phases after dissolution of primary lithiophosphate by hydrothermal solutions.

Physical Properties

The initial crystal of wopmayite was a corroded colorless to white {1011} rhomb ~150 microns across. For characterization, the rhomb was disaggregated, producing water-clear and very gemmy fragments with no visible twinning. Wopmayite is colorless to white to pale pink with a white streak and a vitreous luster, and does not fluoresce under ultraviolet light. It has a Mohs hardness of 5, is brittle, has an irregular to subconchoidal fracture, and shows no cleavage or parting. The density could not be measured because of the paucity of available material; the calculated density is 3.027 g/cm^3. Optical properties were measured with the Bloss spindle stage for the wavelength 590 nm using a gel filter. Wopmayite is uniaxial (–), ω = 1.617, ε = 1.613, both ± 0.002.

Infrared Spectroscopy

Fourier-transform infrared (FTIR) spectra were collected using a Bruker Hyperion 2000 IR microscope equipped with a liquid-nitrogen-cooled MCT detector. Spectra over the range 4000–650 cm^{-1} were obtained by averaging 100 scans with a resolution of 4 cm^{-1}. The IR spectrum shows strong bands at 2830 and 2395 cm^{-1}, labeled A and B in the two spectra in Figures 1a and b. These bands are characteristic of principal (P) O–H stretches (Chapman & Thirlwell 1964) where the

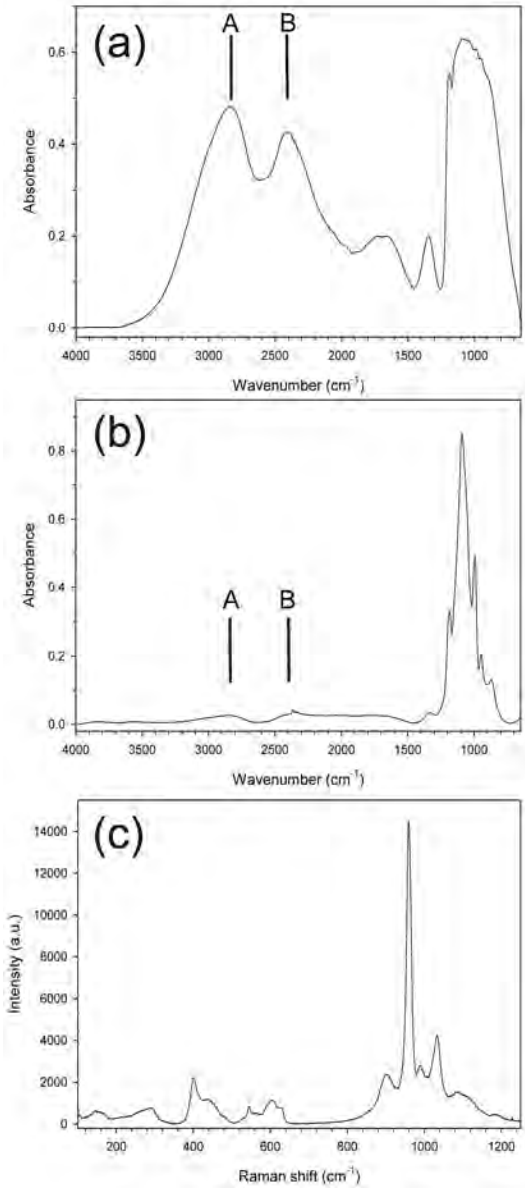

Fig. 1. Infrared and Raman spectra of wopmayite; (a) single-crystal (unpolarized) infrared spectrum; (b) infrared spectrum (diamond press, spot size ~ 100 μm); (c) Raman spectrum.

H atom is involved in strong hydrogen bonding, as is the case in wopmayite. According to Chapman & Thirlwell (1964), the fundamental (P)O–H stretching vibrations occur in the range 3000–2700 cm^{-1} (designated as band A). They also observed a weak-to-medium-intensity band at ~2300–2400 cm^{-1} (designated as band B), which increases in intensity with increase in the number of (P)OH groups in the structure; they assigned this band to (P)O–H stretches. However, Moraes *et al.* (2006) assigned this band to an overtone of the P–O modes. It is of interest to compare the infrared spectrum of wopmayite with that of whitlockite (Figs. 2a,b). In Figure 2a, the spectrum of wopmayite in the 4000–2000 cm^{-1} region is superimposed on the whitlockite spectrum. In whitlockite, there is one distinct (PO_3OH) group involving P at the *P*(3) site, and the associated (OH) group gives rise to peak A_3 (~2950 cm^{-1}) in the IR spectrum of whitlockite. In wopmayite, there are two symmetrically distinct (PO_3OH) groups involving P at the *P*(1) and *P*(3) sites, and the associated (OH) groups gives rise to peaks A_1 (~2830 cm^{-1}) and A_3 (which appears as a shoulder at ~2950 cm^{-1} on the 2830 cm^{-1} peak) in the IR spectrum of wopmayite. Medium-intensity bands at 1720 and 1651 cm^{-1} are assigned to combinations, and a sharp band at 1345 cm^{-1} can be assigned to P–O–H bending vibrations. The bands (that saturate in the single-crystal spectrum, Fig. 1a) at 1185 (s), 1090 (s), 994 (w), and 947 (w) cm^{-1} may be assigned to various stretching bands of the (PO_4) group. A weak band at 870 (w) cm^{-1} is assigned to the P–OH stretching vibration.

Raman Spectroscopy

Raman spectra were collected in back-scattered mode with a HORIBA Jobin Yvon-LabRAM ARAMIS integrated confocal micro-Raman system equipped with a 460 mm focal length spectrograph and a multichannel air-cooled (–70°C) CCD detector. A magnification of 100× was used with an estimated spot size of 1 μm, a 1800 gr/mm grating, an excitation radiation of 532 nm, and a laser power between 5 and 12.5 mW. Calibration was done using the 520.7 cm^{-1} line of Si metal. The Raman spectrum of wopmayite is shown in Figure 1c. In the 850–1150 cm^{-1} region, there are prominent peaks that may be assigned to various P–O stretching modes. Lower-energy peaks from 400–650 cm^{-1} may be assigned to O–P–O deformation modes. In whitlockite (Fig. 2c), the pattern is broadly similar to that of wopmayite, except that some of the bands are significantly broader in wopmayite due to the more extensive positional disorder of (PO_3OH) and (PO_4) groups.

Chemical Composition

Wopmayite was analyzed with a Cameca SX-100 electron microprobe operating in wavelength-dispersion mode with an accelerating voltage of 15 kV, a specimen current of 10 nA, and a beam diameter of 10 μm. The following standards were used: marićite (P), andalusite (Al), fayalite (Fe), spessartine (Mn), forsterite (Mg), diopside (Ca), synthetic $SrTiO_3$ (Sr), and albite (Na). Silicon, S, K, Zn, As, Rb, Y, Cs, Ba, REE, and Pb

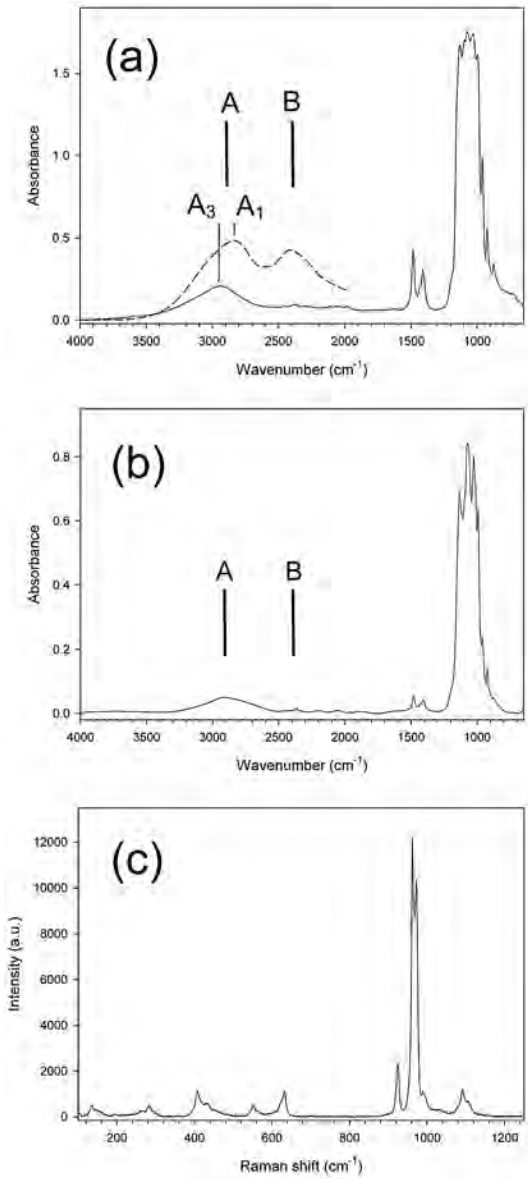

FIG. 2. Infrared and Raman spectra of whitlockite; (a) single-crystal (unpolarized) infrared spectrum, along with the spectrum of wopmayite in the 4000-2000 cm^{-1} region (dashed line); (b) infrared spectrum (diamond press, spot size ~100 μm); (c) Raman spectrum.

were sought but not detected. Back-scattered-electron imaging of the crystal surface revealed a complex pattern of oscillatory zoning that could be related to the variation in Na and Ca content. A weighted mean chemical composition was developed from eight individual point analyses and a visual assessment of the zoning. The data were reduced and corrected by the *PAP* method of Pouchou & Pichoir (1985) and are given in Table 1. The presence and quantity of (OH) groups were established by crystal-structure solution and refinement. In addition, infrared spectroscopy (Figs. 1, 2) shows broad intense bands in the region ~2300–3200 cm^{-1}, indicative of (OH) which is participating in strong hydrogen-bonding. Table 1 gives the chemical composition (weighted mean of eight determinations). The empirical formula was calculated on the basis of 28 O *apfu*: $(Ca_{7.19}\ Na_{1.88}\ Sr_{0.09})_{\Sigma 9.16}(Mn_{0.56}\ Mg_{0.11}Fe^{2+}_{0.14}\ Fe^{3+}_{0.11}Al_{0.08})_{\Sigma 1.00}(PO_4)_{4.63}(PO_3OH)_{2.37}$, with the (OH) content derived as described later.

X-Ray Powder Diffraction

X-ray powder-diffraction data were obtained using a Gandolfi attachment mounted on a Bruker D8 rotating-anode Discover SuperSpeed micro-powder diffractometer with a multi-wire 2D detector. Data (in Å for Cu*K*α) are listed in Table 2. Unit-cell parameters refined from the powder data using CELREF (Appleman & Evans 1973) are as follows: a = 10.370(3), c = 37.085(15) Å, V = 3453.6(17) $Å^3$.

Crystal-Structure Solution And Refinement

A single crystal (40 × 60 × 80 μm) was attached to a tapered glass fiber and mounted on a Bruker D8 three-circle diffractometer equipped with a rotating anode generator (Mo*K*α X-radiation), a multi-layer optics incident-beam path, and an APEX-II CCD detector. In excess of a sphere of X-ray diffraction data (42,095 reflections) was collected to 60° 2θ using 2 s per 0.2° frame with a crystal-to-detector distance of 5 cm. Unit-cell parameters were obtained by least-squares refinement of 9921 reflections with $I > 10\sigma(I)$ and are given in Table 3, together with other information pertaining to data collection and structure refinement. Empirical absorption corrections (SADABS; Sheldrick 2008) were applied and identical data merged to give 12,637 reflections covering the entire Ewald sphere.

TABLE 1. CHEMICAL COMPOSITION OF WOPMAYITE

Constituent	wt.%	Range	Cation	*apfu*
P_2O_5	46.40(16)	46.14–46.61	P	7.00
Al_2O_3	0.38(8)	0.28–0.55		
Fe_2O_3*	0.80		Al	0.08
FeO	0.96	0.61–2.17	Fe^{3+}	0.11
MnO	3.7(3)	3.35–4.56	Mn^{2+}	0.56
MgO	0.41(13)	0.23–0.71	Fe^{2+}	0.14
CaO	37.6(1.1)	35.54–40.01	Mg	0.11
SrO	0.91(16)	0.71–1.26	**Sum *M***	**1.00**
Na_2O	5.4(7)	3.96–6.87		
H_2O**	2.00		Ca	7.19
Total	**98.68**		Na	1.88
			Sr	0.09
			Sum *Ca*, *X*	**9.16**
			(OH)	2.37

* Calculated using structure refinement;
** Calculated on the basis of 28 anions with (OH) = 2.37 *apfu*.

All calculations were done with the SHELXTL PC (Plus) system of programs; R indices are of the form given in Table 3 and are expressed as percentages. The crystal structure was solved by direct methods in the space group $R3c$ and refined to convergence at a final R_1 index of 2.21% by full-matrix least-squares with anisotropic-displacement parameters on all atoms. The refinement procedure will be described below where we discuss the stereochemistry of the structure, as these issues are strongly coupled. We transformed the structure to the coordinates used by Calvo & Gopal (1975), but found the commonly used site-labels for the whitlockite-like minerals cumbersome, and used a simpler labeling scheme (Table 4). Many reflections violating the *c*-glide symmetry operation ($h\,\bar{h}\,l$, l = odd) were observed ($F^2 > 5\sigma$) and several could be identified on precession slices generated from the data frames; however, the intensities of these violating reflections do not adhere to 3-fold symmetry. As will be discussed later, partial local order involving (PO_3OH) and (PO_4) groups may give rise to these weak reflections. Atom positions and anisotropic-displacement parameters are given in Table 4, selected interatomic distances in Table 5 and refined site-scattering values (Hawthorne *et al.* 1995) and assigned site-populations in Table 6. A table of structure-factors and a cif file may be obtained from The Depository of Unpublished Data, on the MAC website [document Wopmayite CM51_93].

Crystal Structure

Coordination of cations and occupancy of cation sites

In the structure of wopmayite, there are four *P* sites that are tetrahedrally coordinated by four O anions at mean distances of 1.538, 1.538, 1.548, and 1.527 Å, respectively, characteristic of P^{5+}. The refined site-scattering values (Table 6) and equivalent-isotropic-displacement parameters of the *P*(1) and *P*(2) sites are in accord with full occupancy of these sites by P, and their <*P*–O> distances are close to the grand <P–O> distance of 1.537 Å given for phosphate minerals by Huminicki & Hawthorne (2002). The <*P*(3)–O> and <*P*(4)–O> distances are in accord with the *P*(3) and *P*(4) sites being occupied by P, but the refined site-scattering values for these sites (Table 6) are significantly less than

TABLE 2. X-RAY POWDER-DIFFRACTION DATA FOR WOPMAYITE

I	$d_{(meas.)}$ (Å)	$d_{(calc.)}$ (Å)	*h*	*k*	*l*	I	$d_{(meas.)}$ (Å)	$d_{(calc.)}$ (Å)	*h*	*k*	*l*
31	8.017	8.082	0	1	2	4	2.087	2.088	$\bar{1}$	3	14
32	6.421	6.451	$\bar{1}$	1	4	8B	2.057*	2.060	0	2	16
33	5.166	5.185	$\bar{1}$	2	0	″	″	2.057	$\bar{3}$	5	1
9	4.355	4.364	$\bar{2}$	2	2	″	″	2.048	$\bar{2}$	5	2
7	4.129	4.119	0	1	8	13	2.019	2.021	0	4	8
16	4.033	4.041	0	2	4	6	1.987	1.986	$\bar{2}$	4	12
29	3.425	3.428	$\bar{1}$	1	10	22	1.920	1.921	$\bar{4}$	4	10
7	3.343	3.339	$\bar{1}$	3	2	13	1.881	1.883	$\bar{2}$	5	8
88	3.186	3.187	$\bar{2}$	3	4	15	1.870	1.868	$\bar{4}$	5	6
10	2.991	2.993	0	3	0	″	″	1.868	$\bar{1}$	5	6
100	2.858	2.859	0	2	10	3	1.817	1.816	0	1	20
27	2.736	2.739	$\bar{1}$	3	8	6	1.801	1.801	$\bar{3}$	5	10
7	2.695	2.694	$\bar{3}$	3	6	12	1.765	1.763	0	5	4
″	″	2.694	0	3	6	28	1.715	1.714	$\bar{2}$	2	20
7	2.652	2.655	$\bar{1}$	2	12	9	1.698	1.697	$\bar{3}$	3	18
68	2.589	2.592	$\bar{2}$	4	0	″	″	1.697	0	3	18
8	2.536	2.537	0	1	14	″	″	1.697	$\bar{1}$	4	16
9	2.500	2.504	$\bar{2}$	3	10	9	1.674	1.675	$\bar{5}$	5	8
7	2.390	2.392	$\bar{1}$	3	11	5	1.627	1.626	$\bar{2}$	5	14
″	″	2.391	$\bar{2}$	4	6	5B	1.616*	1.613	$\bar{4}$	4	16
4	2.363	2.361	$\bar{3}$	4	5	6B	1.593*	1.589	$\bar{5}$	6	4
11	2.240	2.244	$\bar{1}$	1	16	10	1.543	1.543	$\bar{2}$	6	10
12	2.182	2.182	$\bar{4}$	4	4	″	″	1.540	$\bar{3}$	5	16
12	2.150	2.150	$\bar{3}$	3	12						
″	″	2.150	0	3	12						

B = broad reflection
* Not used in least-squares refinement.

TABLE 3. MISCELLANEOUS REFINEMENT DATA FOR WOPMAYITE

a (Å)	10.3926(2)
c	37.1694(9)
V (Å^3)	3476.7(2)
Space group	*R*3*c*
Z	6
$D_{calc.}$ (g/cm^3)	3.027
Radiation/ filter	Mo*K*α/graphite
2θ-range for data collection (°)	60.00
Reflections collected	42095
Reflections in Ewald sphere	12637
Independent reflections	2292
$F_o > 4\sigma F$	2288
Refinement method	Full-matrix least squares on F^2
R(merge) %	1.96
Final $R_{(obs)}$ (%) [$F_o > 4\sigma F$]	R_1 = 2.21
R indices (all data) (%)	R_1 = 2.22 wR_2 = 5.99 GooF = 1.126

$R_1 = \Sigma(|F_o|-|F_c|) / \Sigma|F_o|$
$wR_2 = [\Sigma w(F_o^2 - F_c^2)^2 / \Sigma(F_o^2)^2]^2$, $w = 1/[\sigma^2(F_o)^2 + (0.0279\ P)^2 + (14.20\ P)]$, where $P = (Max(F_o^2,0) + 2\ F_c^2) / 3$

that expected for full occupancy by P. The *P*(3) and *P*(4) sites are too close (0.925 Å, Table 5) for them both to be locally occupied, and the sum of the site-scattering values at these sites (Table 6) is in accord with either *P*(3) or *P*(4) being locally occupied. Thus the site-scattering refinement was constrained such that the sum of their occupancies by P was equal to unity. The O(9) anion is bonded solely to the *P*(3) cation (not counting H atoms) and the occupancy of O(9) was constrained to be the same as that of the *P*(3) site (Table 6). The O(11) anion has very low occupancy (Table 6) and was constrained to have the same occupancy as the *P*(4) site; thus O(11) is vacant where not locally associated with an occupied *P*(4) site. The *P*(4) and O(11) sites are located on the 3-fold axis with refined site-occupancies of 0.15. The remaining anion, O(12), that completes the tetrahedral coordination of the *P*(4) site occurs off the 3-fold axis, and is expected to be very close to the O(10) anion site. In two Palermo whitlockite structures with *P*(4) site-occupancies of 0.19 and 0.27, respectively, the basal O(12) anion of the *P*(4) tetrahedron is 0.33 and 0.31 Å, respectively, from the O(10) anion that belongs to the *P*(3) tetrahedron (Calvo & Gopal 1975, Hughes *et al*. 2008). For wopmayite, we were unable to resolve the O(12) anion from the O(10) anion; the O(10) refined

TABLE 4. ATOM POSITIONS AND DISPLACEMENT PARAMETERS (Å^2) FOR WOPMAYITE

atom	label*	*x*	*y*	*z*	U_{11}	U_{22}	U_{33}	U_{23}	U_{13}	U_{12}	U_{eq}
M	*M*	0	0	0	0.0090(2)	0.0090(2)	0.0090(3)	0	0	0.00450(11)	0.00901(19)
Ca(1)	*Ca*(IIB1)	0.28367(6)	0.14635(6)	0.56677(3)	0.0127(3)	0.0114(2)	0.0114(2)	–0.00247(17)	–0.00174(17)	0.0069(2)	0.01148(16)
Ca(2)	*Ca*(IIB2)	0.39191(6)	0.18197(6)	0.76755(3)	0.0120(3)	0.0105(3)	0.0123(2)	–0.00080(19)	–0.00306(17)	0.0056(2)	0.01160(16)
Ca(3)	*Ca*(IB)	0.28110(10)	0.14942(9)	0.67411(4)	0.0422(5)	0.0273(4)	0.0288(4)	–0.0129(3)	–0.0157(3)	0.0255(4)	0.0292(3)
P(1)	*P*(B1)	0.31498(8)	0.14281(8)	0.86592(3)	0.0104(3)	0.0103(3)	0.0100(3)	0.0001(2)	–0.0001(2)	0.0059(2)	0.00993(14)
P(2)	*P*(B2)	0.35226(8)	0.15731(8)	0.96824(3)	0.0103(3)	0.0106(3)	0.0097(2)	0.0010(2)	0.0006(2)	0.0054(3)	0.01012(13)
P(3)	*P*(A)	0	0	0.75840(4)	0.0088(4)	0.0088(4)	0.0148(6)	0	0	0.0044(2)	0.0108(4)
P(4)	*P*(A′)	0	0	0.7335(2)	0.0088(4)	0.0088(4)	0.0148(6)	0	0	0.0044(2)	0.0108(4)
X	*Ca*(IIA′)	0	0	0.8136(15)	0.065(14)	0.065(14)	0.19(5)	0	0	0.033(7)	0.11(2)
O(1)	O(IB1)	0.2707(2)	0.0955(3)	0.82566(6)	0.0211(9)	0.0267(10)	0.0093(7)	–0.0017(7)	–0.0009(7)	0.0124(8)	0.0188(4)
O(2)	O(IIB1)	0.2430(3)	0.2298(3)	0.87911(6)	0.0258(10)	0.0264(10)	0.0190(9)	–0.0000(7)	0.0023(7)	0.0214(9)	0.0200(4)
O(3)	O(IIB3)	0.2717(2)	0.0003(2)	0.88666(5)	0.0148(8)	0.0118(8)	0.0127(7)	0.0020(6)	0.0009(6)	0.0044(7)	0.0141(3)
O(4)	O(IIB5)	0.4854(2)	0.2409(2)	0.86853(6)	0.0127(9)	0.0131(8)	0.0210(9)	0.0008(7)	0.0005(7)	0.0053(7)	0.0161(4)
O(5)	O(IIB2)	0.3979(2)	0.0463(2)	0.95471(6)	0.0233(10)	0.0229(9)	0.0149(8)	–0.0016(7)	0.0010(7)	0.0165(8)	0.0182(4)
O(6)	O(IIB4)	0.4170(3)	0.3017(2)	0.94682(6)	0.0256(10)	0.0148(9)	0.0193(9)	0.0075(7)	0.0036(7)	0.0071(8)	0.0213(4)
O(7)	O(IIB6)	0.1808(2)	0.0807(2)	0.96383(6)	0.0131(8)	0.0146(8)	0.0161(8)	–0.0016(7)	–0.0018(7)	0.0075(7)	0.0144(4)
O(8)	O(IB2)	0.3998(2)	0.1948(2)	0.00773(6)	0.0220(10)	0.0191(9)	0.0125(8)	–0.0004(7)	–0.0036(7)	0.0112(8)	0.0175(4)
O(9)	O(IA)	0	0	0.8022(2)	0.026(2)	0.026(2)	0.022(2)	0	0	0.0128(11)	0.0245(14)
O(10)	O(IIA)	–0.0165(2)	0.1312(2)	0.74664(6)	0.0194(11)	0.0127(8)	0.0288(10)	0.0048(7)	0.0072(8)	0.0098(8)	0.0195(5)
O(11)	O(IA′)	0	0	0.6931(9)							0.034(8)
O(12)	O(IIA′)										

* Previous labeling of Calvo & Gopal (1975)

TABLE 5. SELECTED INTERATOMIC DISTANCES (Å) IN WOPMAYITE

P(1)–O(1)	1.571(2)	*P*(2)–O(5)	1.535(2)	*P*(3)–O(9)	1.628(7)
P(1)–O(2)	1.515(2)	*P*(2)–O(6)	1.527(2)	*P*(3)–O(10),i,j ×3	1.521(2)
P(1)–O(3)	1.525(2)	*P*(2)–O(7)	1.555(2)	< *P*(3)–O>	1.548
P(1)–O(4)	1.542(2)	*P*(2)–O(8)a	1.536(2)		
<*P*(1)–O>	1.538	<*P*(2)–O>	1.538	*P*(4)–O(11)	1.50(4)
				P(4)–O(10),i,j ×3	1.536(3)
				<*P*(4)–O>	1.527
Ca(1)–O(2)b	2.823(2)	*Ca*(2)–O(1)	2.434(2)	*Ca*(3)–O(1)f	2.679(2)
Ca(1)–O(3)c	2.511(2)	*Ca*(2)–O(2)e	2.401(2)	*Ca*(3)–O(2)e	2.453(2)
Ca(1)–O(4)b	2.519(2)	*Ca*(2)–O(3)f	2.357(2)	*Ca*(3)–O(3)f	2.390(2)
Ca(1)–O(4)c	2.539(2)	*Ca*(2)–O(5)f	2.661(2)	*Ca*(3)–O(5)c	2.406(2)
Ca(1)–O(5)c	2.437(2)	*Ca*(2)–O(6)e	2.673(2)	*Ca*(3)–O(6)b	2.697(2)
Ca(1)–O(6)b	2.316(2)	*Ca*(2)–O(7)f	2.439(2)	*Ca*(3)–O(8)g	2.439(2)
Ca(1)–O(8)d	2.431(2)	*Ca*(2)–O(7)e	2.447(2)	*Ca*(3)–O(8)h	2.500(2)
Ca(1)–O(10)e	2.455(2)	*Ca*(2)–O(10)i	2.375(2)	*Ca*(3)–O(11)	2.628(9)
<*Ca*(1)–O>	2.504	<*Ca*(2)–O>	2.473	<*Ca*(3)–O>	2.524
M–O(4) ×3	2.091(2)	*X*–O(1),i,j ×3	2.512(10)	*P*(3)–*P*(4)	0.925(8)
M–O(7) ×3	2.113(2)	*X*–O(10),i,j ×3	2.88(5)	*X*–O(9)	0.42(6)
<*M*–O>	2.102	<*X*–O>	2.696	*X*–*P*(3)	2.05(5)

a: *x*, *y*, 1+*z*; b: –*x*+*y*+⅔, –*x*+⅔, *z*–⅓; c: –*y*+⅓, *x*–*y*–⅓, *z*–⅓; d: *x*, *x*–*y*, *z*+½; e: –*y*+⅔, –*x*+⅓, *z*–$^1/_6$; f: –*x*+*y*+⅔, *y*+⅓, *z*–$^1/_6$; g: –*x*+*y*+⅓, –*x*+⅔, *z*+⅔; h: –*y*+⅓, *x*–*y*–⅓, *z*+⅔; i: –*x*+*y*, –*x*, *z*; j: –*y*, *x*–*y*, *z*.

to full occupancy and its displacement parameters are analogous to those of the other phosphate anions. We therefore conclude that the O(12) and O(10) sites are not resolvable for the wopmayite crystal studied. We have chosen to include the *P*(4)–O(10) distance of 1.536 Å for the *P*(4) tetrahedron, and recognize that the <*P*(4)–O> value of 1.527 Å is shorter than expected, due to the fact that we were unable to locate a distinct O(12) anion.

TABLE 6. REFINED SITE-SCATTERING VALUES AND ASSIGNED SITE-POPULATIONS IN WOPMAYITE

	Refined site-scattering (*epfu*)	Coordination number and mean bond-length (Å)	Assigned site-populations (*apfu*)	Effective site-scattering (*epfu*)
P(1)	45	[4] 1.538	3.00 P	45
P(2)	45	[4] 1.538	3.00 P	45
P(3)	12.78(9)	[4] 1.548	0.85 P	12.8
P(4)	2.21(9)	[4] 1.527	0.15 P	2.2
M	21.78(9)	[6] 2.102	0.56 Mn^{2+} + 0.11 Fe^{3+} + 0.14 Fe^{2+} + 0.11 Mg + 0.08 Al	22.9
Ca(1)	59.16(18)	[8] 2.504	2.91 Ca + 0.09 Na	59.2
Ca(2)	58.56(18)	[8] 2.473	2.84 Ca + 0.16 Na	58.6
Ca(3)	49.02(18)	[8] 2.524	1.78 Ca + 1.22 Na	49.0
X	2.22(18)	[6] 2.696	0.80 □ + 0.20 Na	2.2
Σ	**169.0**			**169.0**
O(9)	6.82(9)		0.85 O	6.8
O(11)	1.18(9)		0.15 O	1.2

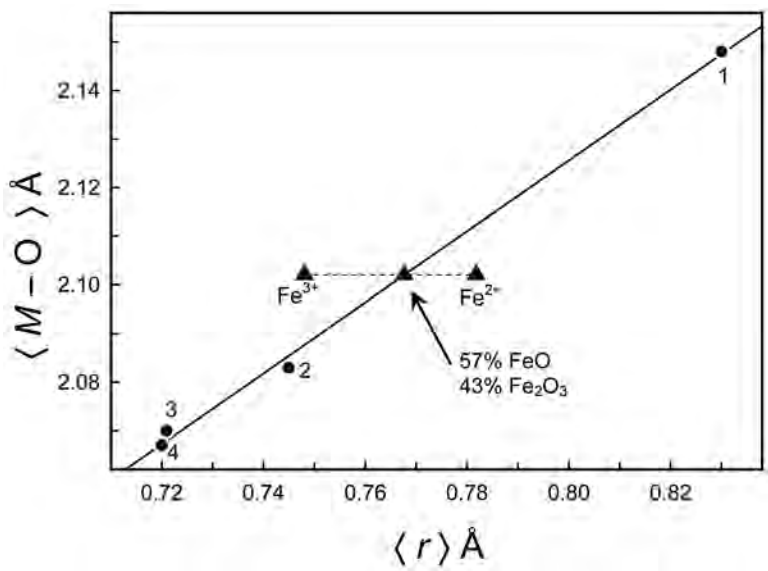

FIG. 3. Variation in <*M*–O> bond-length as a function of aggregate constituent-cation radius for 1: synthetic manganese whitlockite (Kostiner & Rea 1976); 2: Palermo whitlockite (Calvo & Gopal 1975); 3: Tip Top whitlockite (Hughes *et al.* 2008); 4: synthetic whitlockite (Gopal *et al.* 1974), all black circles. Data for wopmayite are shown by black triangles, and the aggregate radii were calculated for all Fe as Fe^{2+}, all Fe as Fe^{3+}, and the Fe^{2+} and Fe^{3+} contents adjusted for colinearity with the line through the other data points.

There is one *M* site that is octahedrally coordinated by six O anions at a mean distance of 2.102 Å. Preliminary normalization of the chemical composition gave the following approximate composition for the *M* site: $Mn_{0.56}Fe_{0.25}Mg_{0.11}Al_{0.08}$. The next issue to be addressed is the valence state(s) of Fe. Figure 3 shows the variation in the observed <*M*–O> distances as a function of the aggregate radius of the assigned cations in four well-refined whitlockite structures (shaded circles). The linear relation allows us to assess the aggregate

M-cation radius in wopmayite. The three black triangles at <*M*–O> = 2.102 Å are aggregate radii for the *M* site in wopmayite with Fe calculated as (1) all Fe^{3+}, (2) all Fe^{2+}, and (3) 57% FeO: 43% Fe_2O_3, the latter calculated such that the constituent radius is in accord with the relation for other whitlockite structures (Fig. 3). The effective scattering of the resultant site-population (Table 6) is in reasonable accord with the refined scattering site-scattering of 21.78(9) *epfu* (electrons per formula unit; Hawthorne *et al*. 1995).

There are three *Ca* sites with <*Ca*–O> distances of 2.504, 2.473, and 2.524 Å, respectively. The *Ca*(1) and *Ca*(2) sites are [8]-coordinated [*i.e.*, the spatially unresolved O(10) and O(12) anions together constitute a single ligand]. From Table 5, it seems that *Ca*(3) is also [8]-coordinated, but this is not generally the case. The cations at *Ca*(3) are close to the O(11) site (Table 5); however, the O(11) site has only 15% occupancy by O, and hence *Ca*(3) is 85% [7]-coordinated and 15% [8]-coordinated. Additionally, there is an octahedrally coordinated *X* site with a <*X*–O> distance of 2.696 Å that is occupied by larger cations (*i.e.*, Na, Ca, Sr). The empirical formula derived from the electron-microprobe results (Table 1) indicates that the *X* and *Ca* sites are occupied in aggregate by $(Ca_{7.19}Na_{1.88}Sr_{0.09})_{\Sigma 9.16}$, which gives a total electron count of 167.9 *epfu* (electrons per formula unit). The corresponding total refined site-scattering over the *X* and three *Ca* sites is 169.0 *epfu* (Table 6). As there are three cations available to assign to each of four crystallographic sites, there is no single solution to the cation distribution (Hawthorne 1983b). As the Sr content is quite minor (0.09 *apfu*), we can exclude it without introducing appreciable error. Assigning *Ca* site populations using the refined site-scattering values results in the following site-populations *Ca*(1): $Ca_{2.91}Na_{0.09}$; *Ca*(2): $Ca_{2.84}Na_{0.16}$; *Ca*(3): $Ca_{1.78}Na_{1.22}$ *apfu* (Table 6). Thus there is strong ordering of Na at the *Ca*(3) site, in accord with the longer mean bondlength at that site. The resultant assigned sum for Ca over the three *Ca* sites is 7.53 Ca *apfu*, which exceeds the 7.19 Ca *apfu* available from electron-microprobe analysis. We attribute this discrepancy to the significant Ca-Na zoning in the crystal recognized during electron-microprobe analysis, and suggest that the weighted mean Ca and Na content given in Table 1 should be used only as an approximation to the electron-scattering from the structure refinement.

There is one *X* site with a refined site-scattering value of 2.2(2) *epfu*. The sum of the large cations in wopmayite is 9.16 *apfu* (Table 1), and thus according to the chemical formula of wopmayite, there are 0.16 cations *pfu* available for the *X* site, in accord with occupancy of that site by dominant □ and minor Na (Table 6).

Bond topology

Most of the structure of wopmayite shows a simple isostructural relation to the structures of whitlockite (*e.g.*, Gopal & Calvo 1972, Calvo & Gopal 1975, Gopal *et al*. 1974, Kostiner & Rea 1976) and merrillite (*e.g.*, Hughes *et al*. 2006). Hughes *et al*. (2008) described the structure of both whitlockite and merrillite as a structural unit consisting of an $[M^{2+}(PO_4)_6]$ arrangement that Moore (1973) has designated as a bracelet-and-pinwheel arrangement; this fragment of the structure consists of the *P*(1), *P*(2), *M*, and O(1)–O(8) sites and is topologically the same in the whitlockite, merrillite, and

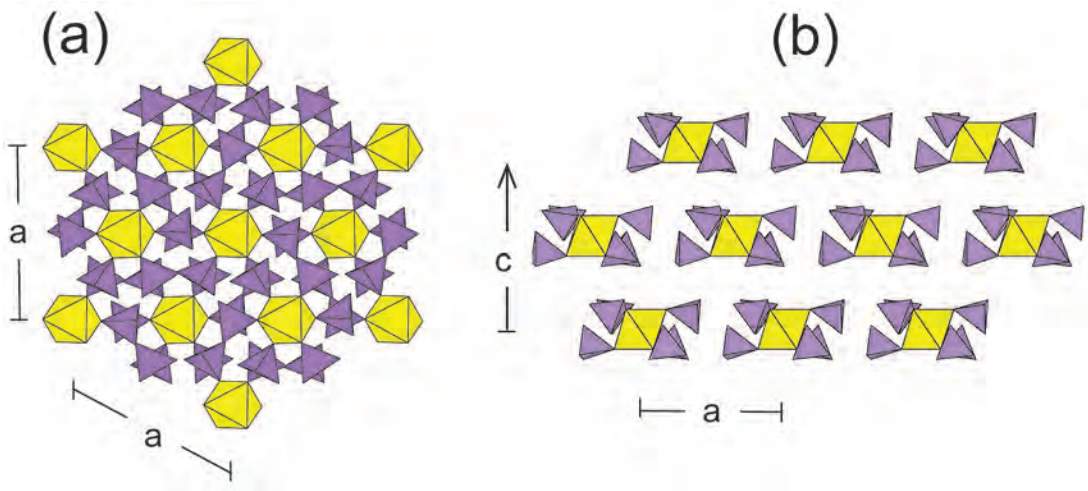

FIG. 4. The $[M(PO_4)_6]$ pinwheel component in the structures of whitlockite, merrillite, and wopmayite: (a) projected onto (001) and (b) projected along [010]. *M* octahedra are yellow, ($P\Phi_4$) groups (Φ = O, OH) are mauve.

wopmayite structures (Fig. 4). The $[M^{2+}(PO_4)_6]$ clusters are linked by Ca polyhedra and $(PO_3\Phi)$ groups of the form $\{Ca_9X(PO_3\Phi)\}$, where Φ = O,OH and X = (□, Na, Ca), depending on the mineral species.

The meaning of the P(3) and P(4) occupancies in merrillite and whitlockite

Gopal & Calvo (1972) showed that heating whitlockite causes it to lose its hydrogen, with the result that the *P*(3), O(9), and O(10) sites are no longer occupied. Hughes *et al.* (2006, 2008) showed that, in the absence of Na, (rare-earth-free) whitlockite and merrillite are related by the substitution

$$^{X}Ca^{m} + \square^{m} = {}^{X}\square^{w} + 2H^{w} \quad (1)$$

where the lower-case superscripts denote the different minerals (m = merrillite, w = whitlockite) and the vacancy in the merrillite structure occurs at the H site. For Na-bearing merrillite, (rare-earth-free) whitlockite and merrillite are related by the substitution

$$^{X}Na^{m} + \square^{m} = {}^{X}\square^{w} + H^{w}. \quad (2)$$

We may write the endmember compositions of merrillite and whitlockite as shown in Table 7, where the phosphate group(s) not involved with the $[M^{2+}(PO_4)_6]$ arrangement is (PO_3OH) in endmember whitlockite and (PO_4) in endmember merrillite. As noted by Hughes *et al.* (2008), the relative occupancies of the *P*(3) and *P*(4) sites indicate the relative amounts of the whitlockite and merrillite components, respectively, in a particular structure.

The meaning of the P(3) and P(4) occupancies in wopmayite

Both components, *P*(3) = (PO_3OH) and *P*(4) = (PO_4), are present in wopmayite, with the former dominant: $[(PO_3OH)_{0.85}\ (PO_4)_{0.15}]$ *pfu* from the refinement; thus endmember wopmayite has (PO_3OH) as the dominant phosphate group not involved with the $[M^{2+}(PO_4)_6]$ arrangement (Table 7). In wopmayite, there is an additional structural mechanism involving $(PO_3OH) \rightarrow (PO_4)$ substitution that couples to extensive Na → Ca replacement. Relative to a whitlockite composition (Table 7), abundant Na enters the structure, replacing Ca. This replacement proceeds with the concomitant addition of H by the substitution

$$^{Ca}Na + H \rightarrow {}^{Ca}Ca + \square \quad (3)$$

that forms acid-phosphate groups that must belong to the $[M^{2+}(PO_4)_6]$ component of the structure, *i.e.*, via protonation of some of the (PO_4) groups involving the *P*(1) and/or *P*(2) sites. The distinction between O and (OH) as tetrahedrally coordinating anions of P can be made by inspection of the bond-valence sums at the O sites. In order to better understand the bond-valence variations at these sites, we used the parameters of Brown & Altermatt (1985) to calculate bond-valence tables for both wopmayite and whitlockite (the Palermo sample from Hughes *et al*. 2008).

In whitlockite, the O(1)–O(8) sites coordinate the *P*(1) and *P*(2) tetrahedra. Each of these O-sites is [4]-coordinated [if one considers the hydrogen bond to O(1) from the (PO_3OH) group at *P*(3)]. However, the relative site multiplicities dictate that only one of the three O(1) anions can receive a hydrogen bond locally [*i.e.*, the (OH) group belonging to the *P*(3) tetrahedron occurs on the three-fold axis, and the O(1) site is situated off the 3-fold axis]. We show this graphically in Figure 5 and in Table 8 by using a 1/3 multiplier for the H(1)…O(1) bond. For Palermo whitlockite (Table 8), the bond-valence sums at O(1) through O(8) range from 1.82 *vu* [for O(1)] to 2.13 *vu*. For any local configuration about O(9), one of the O(1) O atoms receives a hydrogen bond, and the other two O(1) anions do not receive a hydrogen bond; these other two (locally associated) O(1) anions adjust by moving closer to their neighboring cations [*P*(1), *Ca*(2), *Ca*(3)] in order to satisfy their bond-valence requirements in the absence of a hydrogen bond; this disorder results in O(1) and *Ca*(3) having the largest positional-displacement parameters of all the anions O(1)–O(8) and cations *Ca*(1)–C*a*(3), respectively, in Palermo whitlockite (Hughes *et al.* 2008). From a local bond-valence perspective, the Palermo whitlockite structure suggests that, of all the O(1)–O(8) O-atoms belonging to the *P*(1) and *P*(2) phosphate groups, O(1) is the most likely candidate for protonation. Examination of the bond-valence table for wopmayite (Table 9) shows that, for the core structure [*i.e.*, *M*, *Ca*(1), *Ca*(2), *Ca*(3), *P*(1), *P*(2), and O(1)–O(8)], most individual bond-valence values are very similar to their counterparts in Palermo whit-

TABLE 7. EXPANDED ENDMEMBER FORMULAE FOR MERRILITE, WHITLOCKITE AND WOPMAYITE ON A SITE BASIS

Sites	*Ca*(1,2,3)	*X*	*M*	*P*(1)	*P*(2)	*P*(3)	*P*(4)
merrillite	Ca_9	Na	Mg	$(PO_4)_3$	$(PO_4)_3$	□	(PO_4)
whitlockite	Ca_9	□	Mg	$(PO_4)_3$	$(PO_4)_3$	(PO_3OH)	□
wopmayite	$Ca_6\ Na_3$	□	Mn^{2+}	$(PO_3OH)_3$	$(PO_4)_3$	(PO_3OH)	□

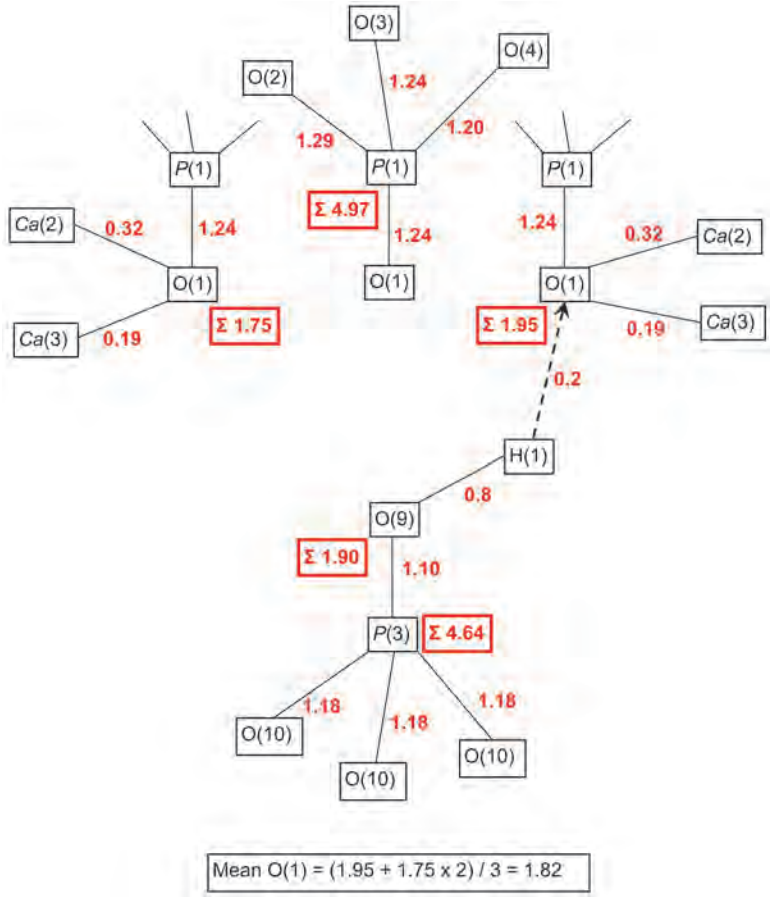

FIG. 5. Sketch of the local hydrogen-bonding associated with the (PO_3OH) group at *P*(3) in Palermo whitlockite; bond-valence values (Table 8) in red.

lockite. However, the bond valence for bonds to O(1) and to *Ca*(3) are significantly less in wopmayite than in Palermo whitlockite. In wopmayite, the O(1) site is further from the *P*(1), *Ca*(2), and *Ca*(3) cations, and all bonds to *Ca*(3) have lower bond-valences (on average) as a result of the significant Na that has replaced Ca at *Ca*(3). The additional bond-valence incident at O(1) [*i.e.*, a hydrogen bond from the H atom attached to O(9) and a donor-H bond to O(1) from a H atom attached to O(1); *i.e.*, the presence of H(2) turns O(1) into an (OH) group] is shown in Figure 6 and entered in the bond-valence table (Table 9) with relative multiplicities assuming a *P*(1) composition of [$(PO_3OH)_2(PO_4)_1$] and a 'maximum whitlockite' *P*(3) composition of (PO_3OH) *pfu*. The bond-valence tables for Palermo whitlockite and wopmayite thus show convincing evidence for the partial occupancy of the *P*(1) tetrahedron [and not the *P*(2) tetrahedron] by (PO_3OH) in wopmayite.

RELATED MINERALS

Wopmayite is structurally related to whitlockite and its homovalent analogues bobdownsite (OH = F) (Tait *et al.* 2011) and strontiowhitlockite (Ca = Sr) (Britvin *et al.* 1991), and merrillite. In the classification of Strunz (Strunz and Nickel 2001), it is a class 8 phosphate (-arsenate-vanadate) of the 8.AC.45 whitlockite group; in the classification of Dana (Gaines *et al.* 1997), it is a class 38 anhydrous normal phosphate (-arsenate-vanadate) related to whitlockite (38.3.4.1) and strontiowhitlockite (38.3.4.2).

CHEMICAL FORMULA

From the expanded formula for wopmayite (Table 7), it is apparent that (PO_3OH) orders at the *P*(1) and

TABLE 8. BOND-VALENCE (*vu*) TABLE FOR PALERMO WHITLOCKITE*

	*M***	*Ca*(1)	*Ca*(2)	*Ca*(3)	*P*(1)	*P*(2)	*Sum*	*P*(3)	*P*(4)	*X*	H(1)	Σ	Σ
O(1)			0.32	0.19	1.24		1.75			0.21$^{x3}\downarrow$	0.2$^{x1/3}\rightarrow$	1.82	1.96
O(2)		0.11	0.27	0.28	1.29		1.95						
O(3)		0.23	0.34	0.32	1.24		2.13						
O(4)	0.38$^{x3}\downarrow$	0.26 0.24			1.20		2.06						
O(5)		0.27	0.16	0.33		1.24	2.00						
O(6)		0.39	0.16	0.15		1.28	1.98						
O(7)	0.35$^{x3}\downarrow$		0.27 0.29			1.20	2.09						
O(8)		0.29		0.27 0.22		1.22	2.00						
Σ		1.79	1.81	1.76									
O(9)								1.10			0.8	1.90	
O(10)		0.24	0.33	0.09				1.18$^{x3}\downarrow$				1.84	
O(11)				0.15$^{x3}\rightarrow$					1.35				1.80
O(12)		0.28	0.33						1.18$^{x3}\downarrow$	0.12$^{x3}\downarrow$			1.91
Σ	2.19	2.03	2.14	1.85	4.97	4.94		4.64	4.89	0.99	1.0		
Σ		2.07	2.14	1.91									

* Labels and values in black are for the dominant whitlockite component of the structure;
labels and values in green are for the minor merrillite component of the structure;
the red values are so-marked to bring them to the readers' attention.
** Using a normalized composition ($Mg_{0.56}Fe^{2+}_{0.30}Fe^{3+}_{0.06}Mn^{2+}_{0.08}$) from Hughes *et al.* (2008, Table 5).

TABLE 9. BOND-VALENCE (*vu*) TABLE FOR WOPMAYITE*

	*M***	*Ca*(1)	*Ca*(2)	*Ca*(3)	*P*(1)	*P*(2)	Sum	*P*(3)	*P*(4)	*X*	H(1)	H(2)	Σ	Σ
O(1)			0.28	0.12	1.13		1.53			0.23$^{x3}\downarrow$	0.2$^{x1/3}\downarrow$	0.8$^{x2/3}\rightarrow$	2.13	1.76
O(2)		0.10	0.31	0.23	1.32		1.96							
O(3)		0.23	0.35	0.27	1.28		2.13							
O(4)	0.41$^{x3}\downarrow$	0.22 0.21			1.22		2.06							
O(5)		0.28	0.15	0.26		1.25	1.94							
O(6)		0.39	0.15	0.12		1.28	1.94							
O(7)	0.38$^{x3}\downarrow$		0.27 0.28			1.18	2.11							
O(8)		0.29		0.23 0.20		1.24	1.96							
Sum		1.72	1.79	1.43										
O(9)								0.97			0.8	0.2$^{x2}\rightarrow$	2.17	
[O(10)]		0.27	0.33	0.05				1.30$^{x3}\downarrow$					1.95	
O11				0.14$^{x3}\rightarrow$					1.37					1.79
[O(12)]		0.27	0.33						1.24$^{x3}\downarrow$	0.08$^{x3}\downarrow$				1.92
Σ	2.37	1.99	2.12	1.48	4.95	4.96		4.87	5.09	0.93	1.0	1.0		
Σ		1.99	2.12	1.57										

* Comments as in the footnote to Table 8 plus the blue label and values for the H(2) site (not located) pertain only to wopmayite in which the *P*(1) tetrahedron = $[(PO_3OH)_2(PO_4)_1]$ *pfu*.
** Using the composition ($Mg_{0.11}Fe^{2+}_{0.14}Fe^{3+}_{0.11}Al_{0.08}Mn^{2+}_{0.56}$).

P(3) sites, the *M* site is dominated by Mn^{2+}, and there is significant Na at the *Ca* sites.

The wopmayite structure is similar to that of whitlockite (*e.g.*, Hughes *et al.* 2008), but differs in two important ways:

(1) there is a noticeable deficit in the refined scattering at the *Ca*(3) site in wopmayite, indicating the presence of a significant amount of a lighter scattering species (*i.e.*, Na from the chemical analysis);

(2) longer cation–O(1) distances in wopmayite indicate significant bond-valence deficiency at O(1).

The largest chemical difference between wopmayite and whitlockite is the dominance of octahedrally coordinated Mn in wopmayite (compared to Mg in whitlockite), and a significant Na content, leading to an average composition near Ca_7Na_2 for the *Ca* sites in wopmayite. The (PO_3OH) content at *P*(3) and (PO_4) content at *P*(4) is given by the respective *P* site occupancies (Hughes *et al.* 2008), which results in a composition of $(PO_3OH)_{0.85}(PO_4)_{0.15}$ for this part of the wopmayite structure. At this stage in the development of the formula for wopmayite, we have an *M* site dominated by divalent cations and a near maximum (PO_3OH) content [*cf.*, whitlockite endmember contains (PO_3OH) = 1], resulting in the simplified formula $Ca_7Na_2Mn^{2+}(PO_4)_6(PO_3OH)$, which carries a charge deficiency of 2. Minor trivalent cations (Fe^{3+}, Al) residing at the *M* site are insufficient to result in electroneutrality, so an additional mechanism is required for this purpose. The most feasible mechanism involves additional (OH) → O substitution at one or more of the O atoms associated with the (PO_4) groups involving the *P*(1) or *P*(2) sites. A comparative bond-valence analysis of the whitlockite (Table 8) and wopmayite (Table 9) structures clearly identifies the O(1) anion in wopmayite as having a significant long-range deficiency in incident

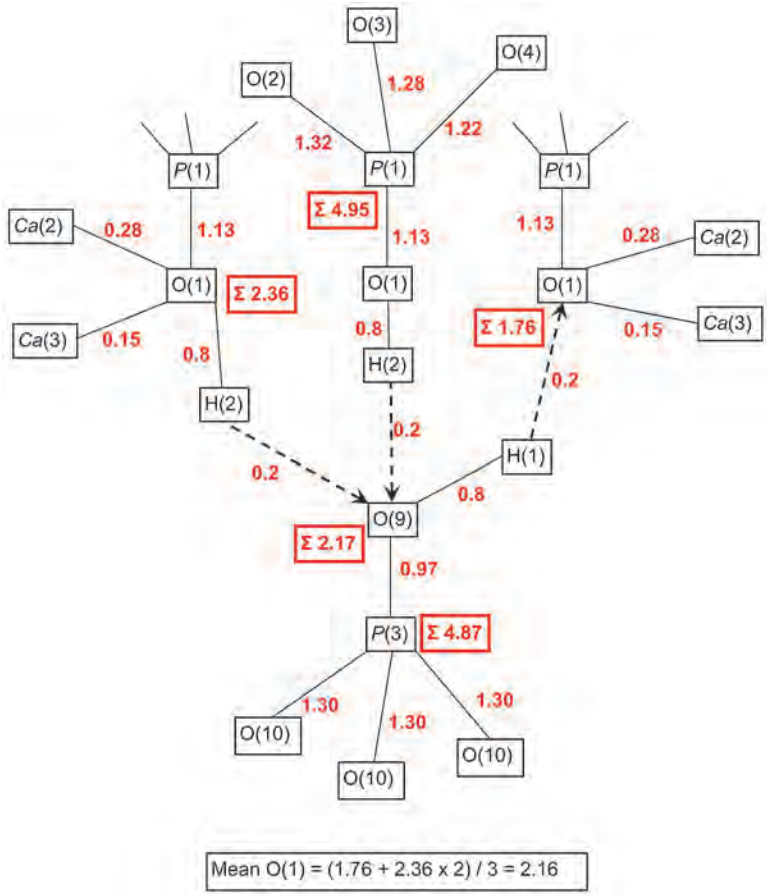

FIG. 6. Sketch of the local hydrogen-bonding associated with the two (PO_3OH) groups and one (PO_4) group at *P*(1) in conjunction with a (PO_3OH) group at *P*(3) in wopmayite; bond-valence values (Table 9) in red.

bond-valence. This indicates that there are different short-range arrangements involving both O and (OH) at O(1) that result in the average incident bond-valence at O(1) in Table 9.

It was not possible to obtain a quantitative measure of the (OH) content at O(1) from the structure refinement alone, and a direct measure of the total H_2O content in wopmayite was not possible given the amount of material available. Hence we assessed the (OH) content at the O(1) site by incrementally increasing the number of (OH) groups in the normalization of the chemical data (28 anions total) and observed the corresponding change in cation stoichiometry. At 2.37 (OH) groups *pfu* [0.85(OH) *pfu* at O(9) and 1.52 (OH) *pfu* at O(1)], we obtained an optimal cation total and ideal stoichiometry (*i.e.*, $M_{1.00}$, $P_{7.00}$), with excellent electron totals at all cation sites (Table 6). The result is an O(1) site occupied by 51% (OH) and 49% O for the average chemical analysis (Na_2O = 5.43 wt.%), and 65% (OH) and 35% O for the composition with the highest Na content (Na_2O = 6.87 wt.%). The structural formula of the wopmayite crystal used for chemical analysis is as follows: $Ca_{7.19}Sr_{0.09}Na_{1.88}\square_{0.84}(Mn^{2+}_{0.56}Fe^{2+}_{0.14}Mg_{0.11}Al_{0.08}Fe^{3+}_{0.11})(PO_4)_{4.63}(PO_3OH)_{2.37}$. In the endmember composition, the *M* site is dominated by Mn^{2+}, the *P*(1) and *P*(3) sites by (PO_3OH), the *P*(2) site by (PO_4), and the *P*(4) and *X* sites by vacancy, and the resulting endmember formula is $Ca_6Na_3\square Mn(PO_4)_3(PO_3OH)_4$. The relations between the endmember formulae of merrillite, whitlockite and wopmayite are shown in Table 7.

The infrared spectrum of whitlockite (Figs. 2a,b) shows a single strong absorption in the fundamental OH-stretching region at ~2950 cm^{-1}, in accord with a single acid phosphate group at the *P*(3) position (Table 7). The infrared spectrum of wopmayite (Figs. 1a,b) shows a strong band in the fundamental OH-stretching region at ~2850 cm^{-1}, corresponding to an acid phosphate group at the *P*(1) position, with a shoulder at ~2950 cm^{-1}, corresponding to an acid phosphate group at the *P*(3) position (the whitlockite component) which shows a weaker hydrogen bond to its acceptor anions than is the case for the acid phosphate group at the *P*(1) position.

Wopmayite: (OH) Content and Paragenetic Sequence

The wopmayite endmember formula is listed in Table 7 with a *P*(1) composition of $(PO_3OH)_3$ and a total of four (OH) groups *pfu*. We have represented the *P*(1) composition as $[(PO_3OH)_2(PO_4)_1]$ in Table 9 and Figure 6 to avoid (1) anomalously short H(1)–H(2) distances, (2) O(1) anions that act as both hydrogen-bond donor and hydrogen-bond receiver, and (3) O(9) anions that would receive three hydrogen-bonds. For wopmayite containing a maximum 'whitlockite component' [*i.e.*, *P*(3) = $(PO_3OH)_1$, *P*(4) = □], if the (PO_3OH) content at *P*(1) is stereochemically limited to a maximum value of two (PO_3OH) groups *pfu*, then the maximum (OH) content in wopmayite may be restricted to a total of three (OH) groups, and the resulting formula is written ideally as $Ca_7Na_2\square Mn(PO_4)_4(PO_3OH)_3$.

Both wopmayite and groatite are Na-(Ca + Mn)-bearing phosphate and acid-phosphate minerals that occur together. The P_2O_5 and Na_2O contents are very similar for both minerals, and they differ most notably in their relative Ca and Mn contents, with Ca > Mn for wopmayite and Mn > Ca for groatite. The (PO_3OH):(PO_4) ratio for groatite is 2:1, and for wopmayite it is closer to 1:1. Groatite occurs as acicular sprays on whitlockite and wopmayite (Cooper *et al.* 2009b). Crystallization seems to have occurred in the sequence whitlockite → wopmayite → groatite, with increasing $[HPO_4]^{2-}$ activity.

Acknowledgements

We thank Tony Kampf and Maxime Baijot for their comments and Associate Editor Frédéric Hatert and Editor Lee Groat for handling the manuscript. This work was supported by a Canada Research Chair in Crystallography and Mineralogy and by Natural Sciences and Engineering Research Council of Canada Discovery, Equipment and Major Installation grants of the Natural Sciences and Engineering Research Council of Canada, and by Innovation grants from the Canada Foundation for Innovation to FCH.

References

Appleman, D.E. & Evans, H.T., Jr. (1973) Job 9214: indexing and least-squares refinement of powder diffraction data. *Geological Survey, Computer Contribution* **20** (NTIS doc. PB2-16188).

Britvin, S.N., Pakhomovskii, Y.A., Bogdanova, A.N., & Skiba, V.I. (1991) Strontiowhitlockite, $Sr_9Mg(PO_3OH)(PO_4)_8$, a new mineral species from the Kovdor deposit, Kola Peninsula, U.S.S.R. *Canadian Mineralogist* **29**, 87–93.

Brown, I.D. & Altermatt, D. (1985) Bond-valence parameters obtained from a systematic analysis of the inorganic crystal structure database. *Acta Crystallographica* **B41**, 244–247.

Calvo, C. & Gopal, R. (1975) The crystal structure of whitlockite from the Palermo Quarry. *American Mineralogist* **60**, 120–133.

Černý, P. (1991) Rare-element granitic pegmatites. I. Anatomy and internal evolution of pegmatite deposits. *Geoscience Canada* **18**, 49–67.

Chapman, A.C. & Thirlwell, L.E. (1964) Spectra of phosphorus compounds - I. The infra-red spectra of orthophosphates. *Spectrochimica Acta* **20**, 937–947.

COOPER, M.A., HAWTHORNE, F.C., & ČERNÝ, P. (2009a) The crystal structure of ercitite, $Na_2(H_2O)_4[Mn^{3+}{}_2(OH)_2(PO_4)_2]$, and its relation to bermanite, $Mn^{2+}(H_2O)_4[Mn^{3+}{}_2(OH)_2(PO_4)_2]$. *Canadian Mineralogist* **47**, 173–180.

COOPER, M.A., HAWTHORNE, F.C., BALL, N.A., RAMIK, R.A., & ROBERTS, A.C. (2009b) Groatite, $NaCaMn^{2+}{}_2(PO_4)[PO_3(OH)]_2$, a new mineral of the alluaudite group from the Tanco pegmatite, Bernic Lake, Manitoba, Canada: Description and crystal structure. *Canadian Mineralogist* **47**, 1225–1235.

FRANSOLET, A.-M., COOPER. M.A., ČERNÝ, P., HAWTHORNE, F.C., CHAPMAN, R., & GRICE, J.D. (2000) The Tanco pegmatite at Bernic Lake, southeastern Manitoba. XV. Ercitite, $NaMn^{3+}PO_4(OH)(H_2O)_2$, a new phosphate mineral species. *Canadian Mineralogist* **38**, 893–898.

GAINES, R.V., SKINNER, H.C.W., FOORD, E.E., MASON, B., & ROSENWIEG, A. (1997) *Dana's New Mineralogy*, Eighth Edition. Wiley and Sons, New York.

GOPAL, R. & CALVO, C. (1972) Structural relationship of whitlockite and β-$Ca_3(PO_4)_2$. *Nature Physical Science* **237**, 30–32.

GOPAL, R., CALVO, C., ITO, J., & SABINE, W.K. (1974) Crystal structure of synthetic Mg-whitlockite, $Ca_{18}Mg_2H_2(PO_4)_{14}$. *Canadian Journal of Chemistry* **52**, 1155–1164.

HAWTHORNE, F.C. (1983a) The crystal structure of tancoite. *Tschermaks Mineralogische Petrographische Mitteilungen* **31**, 121–135.

HAWTHORNE, F.C. (1983b) Quantitative characterization of siteoccupancies in minerals. *American Mineralogist* **68**, 287–306.

HAWTHORNE, F.C., UNGARETTI, L., & OBERTI, R. (1995) Site populations in minerals: terminology and presentation of results of crystal-structure refinement. *Canadian Mineralogist* **33**, 907–911.

HUGHES, J.M., JOLLIFF, B.L., & GUNTER, M.E. (2006) The atomic arrangement of merrillite from the Fra Mauro Formation, Apollo 14 lunar mission: the first structure of merrillite from the Moon. *American Mineralogist* 91, 1547–1552.

HUGHES, J.M., JOLLIFF, B.L., & RAKOVAN, J. (2008) The crystal chemistry of whitlockite and merrillite and the dehydrogenation of whitlockite to merrillite. *American Mineralogist* 93, 1300–1305.

HUMINICKI, D.M.C. & HAWTHORNE, F.C. (2002) The crystal chemistry of the phosphate minerals. *Reviews in Mineralogy and Geochemistry* 48, 123–253.

KOSTINER, E. & REA, J.R. (1976) Crystal structure of manganese whitlockite, $Ca_{18}Mn_2H_2(PO_4)_{14}$. *Acta Crystallographica* **32**, 250–253.

MOORE, P.B. (1973) Bracelets and pinwheels: a topological-geometric approach to the calcium orthosilicates and alkali sulfate structures. *American Mineralogist* 58, 32–42.

MORAES, A.P.A, ROMANO, R., SOUZA FILHO, A.G., FREIRE, P.T.C, MENDES FILHO, J., & ALVES, O.L. (2006) Vibrational spectra of α-$Ge(HPO_4)_2.H_2O$ compound. *Vibrational Spectroscopy* 40, 209–212.

POUCHOU, J.L. & PICHOIR, F. (1985) "PAP" Φ(ρZ) procedure for improved quantitative microanalysis. *In* Microbeam Analysis (J.T. Armstrong, ed.). San Francisco Press, San Francisco, California (104–106).

RAMIK, R.A., STURMAN, B.D., DUNN, P.J., & POVARENNYKH, A.S. (1980) Tancoite, a new lithium sodium aluminum phosphate from the Tanco pegmatite, Bernic Lake, Manitoba. *Canadian Mineralogist* **18**, 185–190

SHELDRICK, G.M. (2008) A short history of *SHELX*. *Acta Crystallographica* **A64**, 112–122.

STILLING, A., ČERNÝ, P., & VANSTONE, P.J. (2006) The Tanco pegmatite at Bernic Lake, Manitoba. XVI. Zonal and bulk compositions and their petrogenetic significance. *Canadian Mineralogist* **44**, 599–623.

STRUNZ, H. & NICKEL, E.H. (2001) *Strunz Mineralogical Tables*, Ninth Edition. Schweizerbart'sche Verlagsbuchhandlung, Stuttgart.

TAIT, K.T., BARKLEY, M.C., THOMPSON, R.M., ORIGLIERI, M.J., EVANS, S.H., PREWITT, C.T., & YANG, H. (2011) Bobdownsite, a new mineral species from Big Fish River, Yukon, Canada, and its structural relationship with whitlockite-type compounds. *Canadian Mineralogist* **49**, 1065–1078.

Received June 5, 2012, revised manuscript accepted January 25, 2013.